Published in final edited form as:
Neuron. 2010 April 15; 66(1): 101–113. doi:10.1016/j.neuron.2010.03.012.

$GABA_B$ receptors modulate NMDA receptor calcium signals in dendritic spines

Jason R. Chalifoux and **Adam G. Carter***
Center for Neural Science, New York University, 4 Washington Place, New York, NY 10003

Summary

Metabotropic $GABA_B$ receptors play a fundamental role in modulating the excitability of neurons and circuits throughout the brain. These receptors influence synaptic transmission by inhibiting presynaptic release or activating postsynaptic potassium channels. However, their ability to directly influence different types of postsynaptic glutamate receptors remains unresolved. Here we examine $GABA_B$ receptor modulation in layer 2/3 pyramidal neurons from the mouse prefrontal cortex. We use two-photon laser-scanning microscopy to study synaptic modulation at individual dendritic spines. Using two-photon optical quantal analysis, we first demonstrate robust presynaptic modulation of multivesicular release at single synapses. Using two-photon glutamate uncaging, we then reveal that $GABA_B$ receptors strongly inhibit NMDA receptor calcium signals. This postsynaptic modulation occurs via the PKA pathway and does not affect synaptic currents mediated by AMPA or NMDA receptors. This novel form of $GABA_B$ receptor modulation has widespread implications for the control of calcium-dependent neuronal function.

Keywords

$GABA_B$ receptor; NMDA receptor; PKA; prefrontal cortex; pyramidal neurons; dendrite; spine; two-photon microscopy; two-photon uncaging

Introduction

GABA is the major inhibitory neurotransmitter in the cortex and signals via both ionotropic and metabotropic receptors (Sivilotti and Nistri, 1991). $GABA_B$ receptors ($GABA_B$-Rs) are G-protein coupled receptors that release both $G_{\alpha\ i/o}$ and $G_{\beta\gamma}$ when activated (Bettler et al., 2004; Mott and Lewis, 1994). These signaling molecules influence many down-stream targets, including inwardly rectifying potassium (K) channels, voltage-sensitive calcium (Ca) channels, and adenylyl cyclase (AC) (Misgeld et al., 1995). $GABA_B$-Rs in the prefrontal cortex

*Corresponding Author: Phone: (212) 998-3882, adam.carter@nyu.edu

Highlights:

- $GABA_B$ receptors decrease presynaptic multivesicular release of glutamate.
- $GABA_B$ receptors inhibit Ca influx but not total current through NMDA receptors.
- $GABA_B$ receptor modulation of NMDA receptor Ca signals is mediated by PKA.

The authors declare that they have no financial conflicts of interests.

are important for higher cognitive processes, including multiple forms of learning and memory (Bowery et al., 2002). They are also therapeutic targets for many neuropsychiatric disorders, including schizophrenia, anxiety, depression and epilepsy (Bettler et al., 1998; Caddick and Hosford, 1996).

Throughout the brain, $GABA_B$-Rs regulate synaptic transmission by either inhibiting neurotransmitter release or dampening postsynaptic excitability. Presynaptic $GABA_B$-Rs inhibit release by modulating Ca channels or interacting with the downstream release machinery (Dittman and Regehr, 1996; Pfrieger et al., 1994; Sakaba and Neher, 2003; Takahashi et al., 1998; Wu and Saggau, 1995). While autoreceptors control release of GABA itself, heteroreceptors regulate the release of other neurotransmitters, including glutamate at excitatory synapses (Dittman and Regehr, 1997; Isaacson et al., 1993). The presence of robust presynaptic modulation at excitatory synapses often makes it difficult to distinguish concurrent postsynaptic effects of $GABA_B$-Rs.

Postsynaptic $GABA_B$-Rs are often located in and near dendritic spines, well positioned to influence glutamate receptors (Beaulieu and Somogyi, 1990; Kulik et al., 2006). Both AMPA receptors (AMPA-Rs) and NMDA receptors (NMDA-Rs) are molecular targets of multiple intracellular signaling cascades (Hollmann and Heinemann, 1994; Leonard and Hell, 1997; Tingley et al., 1997) that can strongly influence their function (Blank et al., 1997; Wang et al., 1994; Westphal et al., 1999). For example, protein kinase A (PKA) can selectively regulate postsynaptic responses mediated by NMDA-Rs (Raman et al., 1996; Skeberdis et al., 2006). However, despite signaling via $G_{\alpha\ i/o}$ and inhibiting PKA (Kaupmann et al., 1998), previous results suggest minimal $GABA_B$-R modulation of postsynaptic glutamate receptors.

Instead, $GABA_B$-Rs primarily dampen postsynaptic excitability by releasing $G_{\beta\gamma}$ subunits to activate inwardly rectifying K channels (Dutar and Nicoll, 1988; Gähwiler and Brown, 1985; Lüscher et al., 1997; Sodickson and Bean, 1996). Opening these channels generates local shunting and slow inhibitory postsynaptic potentials (IPSPs) (Alger, 1984; Benardo, 1994; Newberry and Nicoll, 1984, 1985). These $GABA_B$-R IPSPs can enhance magnesium (Mg) block of NMDA-Rs to indirectly inhibit synaptic responses (Morrisett et al., 1991; Otmakhova and Lisman, 2004). In addition to the direct inhibition of voltage-sensitive Ca channels (Perez-Garci et al., 2006; Sabatini and Svoboda, 2000), this indirect block of NMDA-Rs is thought to be an important mechanism by which $GABA_B$-Rs influence Ca signals in dendrites and spines.

Here we examine the mechanisms by which $GABA_B$-Rs modulate excitatory inputs onto layer 2/3 pyramidal neurons in the prefrontal cortex. Our experiments combine two-photon laser scanning microscopy (2PLSM) with two-photon laser uncaging (2PLU) of glutamate to determine the pre- and post-synaptic influences of $GABA_B$-Rs at single spines. Two-photon optical quantal analysis reveals that presynaptic $GABA_B$-Rs reduce multivesicular release at individual synapses. In addition, 2PLU demonstrates that postsynaptic $GABA_B$-Rs directly modulate NMDA-Rs via the PKA pathway. This effect is specific for NMDA-R Ca signals, with little impact on synaptic currents mediated by either AMPA-Rs or NMDA-Rs. These results demonstrate a novel role for $GABA_B$-Rs in modulating synaptic transmission and Ca signaling in cortical pyramidal neurons. Given the importance of NMDA-R Ca signals for synaptic plasticity, spine morphology, local excitability and disease, these results have widespread functional consequences.

Results

Modulation of synaptic transmission

We assessed the influence of $GABA_B$-R activation on glutamatergic synaptic transmission in the dendrites of layer 2/3 pyramidal neurons in acute prefrontal cortical slices. In our initial experiments, we used 2PLSM and laser-scanning DIC (LS-DIC) to position a theta-glass extracellular stimulus electrode near the basal dendrites, where most synaptic inputs are received (Larkman, 1991) (Figure 1A). In neurons held at −70 mV, local stimulation evoked fast AMPA-R excitatory postsynaptic currents (EPSCs) in the presence of 10 μM CPP to block NMDA-Rs (Figure 1B). These AMPA-R EPSCs were suppressed by bath application of the $GABA_B$-R agonist baclofen (5 μM) (19 ± 3% of baseline, n = 18 cells, $p < 0.01$) (Figures 1C). Similar stimulation in neurons held at +40 mV evoked slow NMDA-R EPSCs in the presence of 10 μM NBQX to block AMPA-Rs (Figure 1B). These NMDA-R EPSCs were also suppressed by wash-in of 5 μM baclofen (23 ± 4% of baseline, n = 11 cells, $p < 0.01$) (Figures 1C). These results indicate that $GABA_B$-Rs modulate synaptic transmission at these neurons, which could occur via pre- or post-synaptic mechanisms.

We found that both AMPA-R and NMDA-R EPSCs undergo paired-pulse facilitation (PPF) at these synapses (Figure 1B). This form of short-term synaptic plasticity is often used as an indicator of changes in presynaptic release probability. Bath application of 5 μM baclofen enhanced PPF of both AMPA-R (125 ± 7% of baseline, n = 18 cells, $p < 0.05$) and NMDA-R (124 ± 6% of baseline, n = 11 cells, $p < 0.01$) EPSCs (Figures 1D). These results suggest that $GABA_B$-Rs act presynaptically to suppress glutamate release, but do not exclude additional effects on postsynaptic glutamate receptors.

Single synapse modulation

We began to distinguish the pre- and post-synaptic effects of $GABA_B$-Rs using two-photon optical quantal analysis (Higley et al., 2009; Oertner et al., 2002). 2PLSM and LS-DIC allowed us to position an extracellular stimulus electrode near a targeted spine in the proximal basal dendrites (Figure 2A). We found that stimulating with theta-glass pipettes (1 - 4 μm tip diameter) provided particularly high spatial resolution and allowed us to reliably select individual spines. In neurons held at +10 mV and in the presence of NBQX to block AMPA-Rs (see Methods), local stimulation evoked slow Ca signals in spines, which were completely blocked by wash-in of 10 μM CPP (0 ± 1% of baseline, n = 4 cells, 4 spines, $p < 0.05$). These NMDA-R Ca signals are similar to those observed in other brain regions, and reflect the release and binding of glutamate from an adjacent presynaptic terminal.

The stochastic nature of synaptic transmission means that some trials show clear successes and others failures (Figure 2B) (Mainen et al., 1999). We measured the probability of release (P_r) at individual spines as the ratio of successes to total stimulus trials, which was 0.80 ± 0.1 (n = 15 spines) in these recording conditions. We also measured the synaptic potency at individual spines as the amplitude of the successful events (see Methods), which was 0.19 ± .02 $\Delta G/G_{sat}$ (n = 15 spines). Measuring changes in P_r and synaptic potency has previously been used to distinguish effects on presynaptic glutamate release and postsynaptic receptor activation by different modulators at other synapses (Higley et al., 2009; Oertner et al., 2002).

Having obtained stable baseline responses, we tested for the effects of $GABA_B$-R modulation by washing baclofen into the bath (Figure 2B). We found that 5 μM baclofen nearly eliminated the NMDA-R Ca signal by dramatically reducing the probability of release (5 ± 6% of baseline, n = 5 cells, 5 spines, $p < 0.01$), indicating powerful $GABA_B$-R modulation at the level of single synapses. However, the absence of successful events after 5 μM baclofen prevented us from separating pre- and post-synaptic influences in these experiments.

In order to distinguish between these influences, we reduced the level of $GABA_B$-R modulation by using a lower concentration of baclofen. We also performed parallel experiments with wash-in of ACSF alone, in order to control for any rundown of synaptic transmission. We found that bath application of 1 μM baclofen influenced release to a degree that allowed us to perform two-photon optical quantal analysis (Figure 3A). As expected, 1 μM baclofen decreased the probability of release, consistent with a presynaptic effect (57 ± 13% of baseline, n = 10 cells, 10 spines, $p < 0.01$; ACSF: 95 ± 8% of baseline, n = 5 cells, 5 spines, $p > 0.05$; ACSF vs. baclofen, $p < 0.01$) (Figure 3B). However, 1 μM baclofen also decreased the synaptic potency, suggesting a postsynaptic influence (59 ± 7% of baseline, n = 10 cells, 10 spines, $p < 0.01$; ACSF: 81 ± 10% of baseline, n = 5 cells, 5 spines, $p > 0.05$; ACSF vs. baclofen, $p < 0.05$) (Figure 3C). Together, these results suggest that $GABA_B$-R modulation may occur at both pre- and post-synaptic targets.

Presynaptic modulation

Even when using two-photon optical quantal analysis, distinguishing between changes in presynaptic release and postsynaptic receptor activation can be difficult. For example, multivesicular release can generate graded postsynaptic responses (Foster et al., 2002; Wadiche and Jahr, 2001), such that changes in release probability can appear as changes in synaptic potency (Higley et al., 2009; Oertner et al., 2002). We next tested whether this presynaptic effect contributes to the observed changes in synaptic potency at these synapses.

$GABA_B$-Rs are metabotropic receptors and modulation involves G-protein coupled signaling cascades (Bettler et al., 2004). Therefore, including the non-hydrolyzable GDP analog GDP-βS in the recording pipette should eliminate postsynaptic modulation, allowing us to isolate presynaptic effects. We repeated the two-photon optical quantal experiments with 3 mM GDP-βS in the recording pipette, but found that 1 μM baclofen caused similar modulation of release probability (55 ± 9% of baseline, n = 10 cells, 10 spines, $p < 0.01$; ACSF: 107 ± 9% of baseline, n = 7 cells, 7 spines, $p > 0.05$; ACSF vs. baclofen, $p < 0.01$) and synaptic potency (56 ± 8% of baseline, n = 10 cells, 10 spines, $p < 0.05$; ACSF: 84 ± 7% of baseline, n = 7 cells, 7 spines, $p > 0.05$; ACSF vs. baclofen, $p < 0.05$) (Figures 4A & 4C). These results suggest a reduction in multivesicular release may indeed contribute to the observed changes in synaptic potency.

Switching from normal (2 mM) to low (1 mM) extracellular Ca reduces the probability of release to 0.30 ± 0.05 (n = 14 spines) and should therefore reduce multivesicular release (Foster et al., 2002; Wadiche and Jahr, 2001). When we repeated these experiments in 1 mM Ca, we found that 1 μM baclofen continued to decrease the release probability (42 ± 10% of baseline, n = 8 cells, 8 spines, $p < 0.01$; ACSF: 98 ± 12% of baseline, n = 6 cells, 6 spines, $p > 0.05$; ACSF vs. baclofen, $p < 0.05$) but no longer significantly decreased the synaptic potency (90 ± 19% of baseline, n = 8 cells, 8 spines, $p > 0.05$; ACSF: 110 ± 12% of baseline, n = 6 cells, 6 spines, $p > 0.05$; ACSF vs. baclofen, $p > 0.05$) (Figures 4B & 4C). Together, these results indicate that in normal (2 mM) extracellular Ca, $GABA_B$-R activation reduces multivesicular release to lower synaptic potency. In contrast, in low (1 mM) extracellular Ca, multivesicular release is already reduced and $GABA_B$-R activation no longer has a presynaptic effect. However, these findings do not preclude an additional role for $GABA_B$-R modulation of postsynaptic glutamate receptors.

Postsynaptic modulation

In order to assess postsynaptic $GABA_B$-R modulation, we used 2PLU to bypass the presynaptic terminal and directly activate glutamate receptors on individual spines (Figure 5A) (Carter and Sabatini, 2004; Matsuzaki et al., 2001). We first isolated 2PLU-evoked NMDA-R Ca signals, recorded while blocking postsynaptic K channels with intracellular cesium (Cs), sodium (Na) channels with TTX, and AMPA-Rs with NBQX (see Methods). In neurons held at +10 mV,

these Ca signals had similar amplitudes (0.16 ± 0.02 $\Delta G/G_{sat}$, n = 42) to those evoked by extracellular stimulation and were also blocked by 10 μM CPP (2 ± 2% of baseline, n = 3 cells, 5 spines, $p < 0.01$). We found that 5 μM baclofen strongly suppressed NMDA-R Ca signals (59 ± 6% of baseline, n = 6 cells, 10 spines, $p < 0.01$; ACSF: 96 ± 8% of baseline, n = 10 cells, 17 spines, $p > 0.05$; ACSF vs. baclofen, $p < 0.01$) (Figures 5B & 5C). A similar trend was also seen with 1 μM baclofen (85 ± 12% of baseline, n = 6 cells, 10 spines, $p > 0.05$; ACSF vs. baclofen, $p > 0.05$) (Figures 5B & 5C), suggesting that some of the synaptic potency decrease in our initial two-photon optical quantal experiments may also be postsynaptic. These results demonstrate that postsynaptic $GABA_B$-Rs can modulate NMDA-Rs to suppress spine Ca signals.

Several additional factors could indirectly contribute to $GABA_B$-R suppression of 2PLU-evoked NMDA-R Ca signals. For example, voltage-sensitive Ca channels (VSCCs) have been shown to influence NMDA-R Ca signals at other synapses (Bloodgood and Sabatini, 2007). In principle, $GABA_B$-Rs could suppress NMDA-R Ca signals by inhibiting these VSCCs (Mintz and Bean, 1993; Scholz and Miller, 1991). Wash-in of a cocktail of VSCC blockers (see Methods) effectively blocked Ca signals evoked by back-propagating action potentials in both dendrites and spines (spine: 8 ± 16% of baseline, dendrite: 4 ± 10% of baseline, n = 3 cells, 5 spine/dendrite pairs, $p < 0.01$) (Figure S1). However, these VSCC blockers had no effect on NMDA-R Ca signals (92 ± 13% of baseline, n = 5 cells, 10 spines, $p > 0.05$; ACSF: 99 ± 12% of baseline, n = 5 cells, 10 spines, $p > 0.05$; ACSF vs. baclofen, $p > 0.05$) (Figure S1). Moreover, performing experiments in these blockers did not prevent modulation by 5 μM baclofen (40 ± 4% of baseline, n = 5 cells, 10 spines, $p < 0.01$; ACSF: 84 ± 10% of baseline, n = 5 cells, 10 spines, $p > 0.05$; ACSF vs. baclofen, $p < 0.01$) (Figures 6A & 6E). These results indicate that postsynaptic VSCCs are not required for $GABA_B$-R modulation of NMDA-R Ca signals.

Postsynaptic $GABA_B$-Rs are usually thought to activate inwardly rectifying K channels, causing a change in membrane potential, altering the amount of Mg block of NMDA-Rs, and thus influencing their Ca signals (Morrisett et al., 1991; Otmakhova and Lisman, 2004). However, performing experiments in 0 mM extracellular Mg had no impact on modulation by 5 μM baclofen (65 ± 5% of baseline, n = 5 cells, 10 spines, $p < 0.01$; ACSF: 84 ± 6% of baseline, n = 5 cells, 10 spines, $p > 0.05$; ACSF vs. baclofen, $p < 0.05$) (Figures 6B & 6E). These results demonstrate that changes in Mg block cannot explain the effects on NMDA-R Ca signals.

Release from internal Ca stores can also influence synaptic NMDA-R Ca signals (Kovalchuk et al., 2000). Consistent with these findings, wash-in of cyclopiazonic acid (CPA) (30 μM), which depletes internal Ca stores, caused a small but significant reduction in NMDA-R Ca signals (73 ± 6% of baseline, n = 5 cells, 10 spines, $p < 0.05$; DMSO: 93 ± 7% of baseline, n = 6 cells, 12 spines, $p > 0.05$; DMSO vs. CPA, $p < 0.05$) (Figure 6C & 6E). However, performing experiments in CPA did not prevent modulation by 5 μM baclofen (75 ± 10% of baseline, n = 5 cells, 10 spines, $p < 0.05$; ACSF: 100 ± 14% of baseline, n = 5 cells, 10 spines, $p > 0.05$; ACSF vs. baclofen, $p < 0.05$) (Figures 6D & 6E). These results indicate that internal Ca stores can contribute to NMDA-R Ca signals but are not required for $GABA_B$-R modulation. Together, these findings suggest that postsynaptic $GABA_B$-Rs influence spine Ca signals by directly modulating NMDA-Rs.

Metabotropic pathways

$GABA_B$-R activation releases both $G_{\beta\gamma}$ subunits that directly inhibit their targets and $G_{\alpha\ i/o}$ subunits that act indirectly via protein kinases (Bettler et al., 2004; Mott and Lewis, 1994). We next tested for the involvement of different signaling pathways by introducing specific blockers to either the whole-cell recording pipette or bathing solution. In the presence of GDP-βS (3 mM) in the recording pipette, 5 μM baclofen no longer had an impact on 2PLU-evoked NMDA-

R Ca signals (96 ± 8% of baseline, n = 5 cells, 10 spines, $p > 0.05$; ACSF: 95 ± 11% of baseline, n = 5 cells, 10 spines, $p > 0.05$; ACSF vs. baclofen, $p > 0.05$) (Figures 7A). This finding demonstrates a role for G-protein signaling in postsynaptic $GABA_B$-R modulation of NMDA-R Ca signals.

NMDA-Rs can be modulated by a variety of protein kinases, including protein kinase A (PKA) and protein kinase C (PKC) (Hollmann and Heinemann, 1994). Previous studies indicate that PKA can modulate Ca influx through NMDA-Rs (Skeberdis et al., 2006). Consistent with these findings, wash-in of the membrane-permeable PKA antagonist H89 (10 μM) reduced NMDA-R Ca signals (54 ± 5% of baseline, n = 5 cells, 10 spines, $p < 0.01$; ACSF: 88 ± 10% of baseline, n = 5 cells, 10 spines, $p > 0.05$; ACSF vs. H89, $p < 0.05$) (Figure 7B & 7F). In the presence of H89 in the bath, 5 μM baclofen no longer impacted NMDA-R Ca signals relative to ACSF controls (87 ± 10% of baseline, n = 6 cells, 12 spines, $p > 0.05$; ACSF: 86 ± 8% of baseline, n = 6 cells, 12 spines, $p > 0.05$; ACSF vs. baclofen, $p > 0.05$) (Figures 7C & 7F). Similarly, in the presence of the PKA inhibitory peptide PKI (100 μM) in the recording pipette, 5 μM baclofen did not reduce NMDA-R Ca signals relative to ACSF controls (72 ± 7% of baseline, n = 5 cells, 10 spines, $p > 0.05$; ACSF: 69 ± 3% of baseline, n = 5 cells, 10 spines, $p > 0.05$; ACSF vs. baclofen, $p > 0.05$) (Figures 7D & 7F). In contrast, in the presence of the PKC inhibitory peptide PKC-I (100 μM) in the recording pipette, 5 μM baclofen continued to suppress NMDA-R Ca signals (44 ± 7% of baseline, n = 5 cells, 10 spines, $p < 0.01$; ACSF: 101 ± 12% of baseline, n = 5 cells, 10 spines, $p > 0.05$; ACSF vs. baclofen, $p < 0.01$), suggesting a limited role for PKC (Figures 7E & 7F). These results indicate that postsynaptic $GABA_B$-Rs modulate NMDA-Rs via the PKA pathway to influence spine Ca signals.

Previous studies suggest that PKA modulation of NMDA-R Ca signals may be saturated under baseline conditions (Skeberdis et al., 2006). Consistent with this, wash-in of the adenylyl cyclase (AC) activator forskolin (50 μM) had no effect on our NMDA-R Ca signals (96 ± 10% of baseline, n = 5 cells, 10 spines, $p > 0.05$; DMSO: 91 ± 12% of baseline, n = 5 cells, 9 spines, $p > 0.05$; DMSO vs. forskolin, $p > 0.05$) (Figure S2). However, pre-incubation with 5 μM baclofen in the bath enabled forskolin to increase NMDA-R Ca signals (128 ± 17% of baseline, n = 7 cells, 14 spines, $p < 0.05$; DMSO: 97 ± 12% of baseline, n = 5 cells, 10 spines, $p > 0.05$; DMSO vs. forskolin, $p < 0.05$) (Figure S2). Thus, forskolin can enhance NMDA-R Ca signals when constitutive activation of the PKA pathway is first reduced by activation of $GABA_B$-Rs.

No modulation of synaptic currents

Postsynaptic modulation of NMDA-Rs may selectively influence Ca permeability more than the total synaptic current (Skeberdis et al., 2006; Sobczyk and Svoboda, 2007). We used 2PLU to test whether $GABA_B$-Rs also modulate synaptic currents mediated by AMPA-Rs and NMDA-Rs. We first isolated AMPA-R uncaging-evoked EPSCs (uEPSCs), recorded while blocking postsynaptic K channels with intracellular Cs, Na channels with TTX, and NMDA-Rs with CPP (see Methods). AMPA-R uEPSCs had similar amplitudes and kinetics to miniature EPSCs (mEPSCs) recorded in the same neurons and were blocked by NBQX (10 μM) (0 ± 1% of baseline, n = 3 cells, 6 spines, $p < 0.01$) (Figure 8A). Wash-in of 5 μM baclofen had no effect on AMPA-R uEPSCs (98 ± 7% of baseline, n = 7 cells, 11 spines, $p > 0.05$; ACSF: 92 ± 11% of baseline, n = 6 cells, 10 spines, $p > 0.05$; ACSF vs. baclofen, $p > 0.05$) (Figure 8B). These results indicate that $GABA_B$-Rs do not modulate AMPA-Rs, consistent with previous results in other neurons measuring the effects of $GABA_B$-Rs on spontaneous and miniature EPSCs (Dittman and Regehr, 1996; Scanziani et al., 1992).

We next isolated NMDA-R uncaging-evoked EPSCs (uEPSCs), recorded while blocking postsynaptic K channels with intracellular Cs, Na channels with TTX, and AMPA-Rs with NBQX (see Methods). As expected, we could not observe NMDA-R uEPSCs in our normal recording conditions, because there was no current at +10 mV. In order to examine NMDA-R

uEPSCs, we first performed experiments at −70 mV to increase the driving force and in 0 mM extracellular Mg to remove block. Under these conditions, wash-in of 5 μM baclofen had no effect on NMDA-R uEPSCs (89 ± 7% of baseline, n = 9 cells, 15 spines, $p > 0.05$; ACSF: 102 ± 15% of baseline, n = 6 cells, 11 spines, $p > 0.05$; ACSF vs. baclofen, $p > 0.05$) but continued to decrease the simultaneously recorded NMDA-R Ca signals (66 ± 8% of baseline, n = 9 cells, 15 spines, $p < 0.01$; ACSF: 110 ± 14% of baseline, n = 6 cells, 11 spines, $p > 0.05$; ACSF vs. baclofen, $p < 0.01$) (Figure 8C). Similar results were found when recording NMDA-R uEPSCs and Ca signals in standard 1 mM extracellular Mg at both −20 mV (uEPSC: 96 ± 14% of baseline, n = 5 cells, 10 spines, $p > 0.05$; ACSF: 107 ± 16% of baseline, n = 5 cells, 10 spines, $p > 0.05$; ACSF vs. baclofen, $p > 0.05$. Ca signal: 52 ± 4% of baseline, n = 5 cells, 10 spines, $p < 0.05$; ACSF: 95 ± 12% of baseline, n = 5 cells, 10 spines, $p > 0.05$; ACSF vs. baclofen, $p < 0.05$) and +40 mV (uEPSC: 92 ± 12% of baseline, n = 5 cells, 10 spines, $p > 0.05$; ACSF: 93 ± 15% of baseline, n = 5 cells, 10 spines, $p > 0.05$; ACSF vs. baclofen, $p > 0.05$. Ca signal: 53 ± 12% of baseline, n = 5 cells, 10 spines, $p < 0.05$; ACSF: 97 ± 14% of baseline, n = 5 cells, 10 spines, $p > 0.05$; ACSF vs. baclofen, $p < 0.05$) (Figure S3). These results indicate that $GABA_B$-Rs do not modulate overall synaptic currents through NMDA-Rs. Instead, $GABA_B$-R modulation is only observed when measuring Ca signals generated in single spines. These findings are consistent with a decrease in the Ca permeability of NMDA-Rs due to inhibition of the PKA pathway (Skeberdis et al., 2006). This selective effect may also explain why this form of $GABA_B$-R modulation has not previously been detected in other studies that did not use these optical approaches.

Discussion

We have shown that $GABA_B$-Rs modulate both pre- and post-synaptic targets to influence synaptic transmission at individual spines. Presynaptic $GABA_B$-Rs indirectly suppress NMDA-R Ca signals by inhibiting multivesicular release and reducing the synaptic glutamate signal. Postsynaptic $GABA_B$-Rs directly suppress NMDA-R Ca signals, without significantly affecting AMPA-R or NMDA-R synaptic currents. This novel and powerful form of postsynaptic $GABA_B$-R modulation depends on G-protein signaling and involves the PKA pathway. NMDA-R Ca signals in neurons are fundamentally important for synaptic plasticity, local excitability, and spine morphological changes. Therefore, their modulation by $GABA_B$-Rs has broad implications for Ca-dependent function throughout the brain.

Postsynaptic modulation

The presence of strong presynaptic modulation at many excitatory synapses has often made it difficult to study simultaneous postsynaptic regulation. The classical approach is to measure the amplitude and time-course of quantal events (Dittman and Regehr, 1996; Scanziani et al., 1992). However, this is usually only possible for AMPA-Rs, because NMDA-R quantal events are too small and spontaneous Ca signals too infrequent. Two-photon glutamate uncaging allowed us to bypass the presynaptic terminal and directly activate both AMPA-Rs and NMDA-Rs (Bloodgood and Sabatini, 2007; Carter and Sabatini, 2004; Carter et al., 2007; Matsuzaki et al., 2001; Sobczyk and Svoboda, 2007). By using voltage-clamp recordings with intracellular Cs and extracellular TTX, we were able to isolate synaptic responses evoked at individual spines. Our results show that postsynaptic $GABA_B$-R activation robustly suppresses NMDA-R Ca signals, independent of any effects on presynaptic release.

Postsynaptic $GABA_B$-R modulation of NMDA-R Ca signals is usually thought to occur through indirect mechanisms. For example, activation of inwardly rectifying K channels can hyperpolarize the membrane, enhance Mg block of NMDA-Rs, and reduce their Ca signals (Morrisett et al., 1991; Otmakhova and Lisman, 2004). However, we observed similar $GABA_B$-R modulation in recording conditions where: 1) neurons were held in voltage-clamp

at different membrane potentials, 2) voltage-sensitive Ca channels (VSCCs) were blocked, 3) extracellular Mg was reduced to 0 mM, and 4) internal Ca stores were depleted with CPA. These manipulations reduce any potential indirect effects on NMDA-R Ca signals, and indicate that modulation is directly onto these receptors. To our knowledge, this form of postsynaptic $GABA_B$-R modulation has not previously been shown, likely because it would be difficult to detect without the combination of optical tools we have used.

Previous studies have shown that $GABA_B$-Rs can inhibit PKA (Kaupmann et al., 1998) and that PKA can modulate Ca influx through NMDA-Rs (Skeberdis et al., 2006). Our results indicate that postsynaptic $GABA_B$-Rs signal via the PKA pathway to directly inhibit NMDA-R Ca signals in dendritic spines. While we rule out a requirement for the PKC pathway in this modulation, the possibility remains that $G_{\beta\gamma}$ subunits and other signaling molecules may also play a role. However, we found that the PKA inhibitors H89 and PKI both occlude the influence of $GABA_B$-R activation, suggesting that the PKA pathway may be sufficient.

PKA has a basal level of activity in neurons, such that both increases and decreases in activity can modulate glutamate receptors (Hollmann and Heinemann, 1994; Raman et al., 1996). The reduction of NMDA-R Ca signals with wash-in of H89 likely reflects block of this steady-state PKA activity. In contrast, the inability of forskolin to increase these signals suggests maximal PKA influence in baseline conditions. Thus, prior reduction of PKA activity with $GABA_B$-R activation allows forskolin to increase NMDA-R Ca signals. In the prefrontal cortex, multiple modulators signal via the PKA pathway, including GABA, dopamine, noradrenaline, serotonin and adenosine. In future experiments, it will be interesting to determine the extent to which these modulators interact to influence Ca signals in dendrites and spines.

In contrast to NMDA-R Ca signals, we observed no influence of $GABA_B$-R activation on AMPA-R or NMDA-R uEPSCs evoked at individual spines. The lack of an effect on these postsynaptic currents suggests that $GABA_B$-Rs selectively modulate the Ca permeability of NMDA-Rs. This finding is in agreement with the selective modulation of Ca influx through these receptors by the PKA pathway (Skeberdis et al., 2006). Because only ~10% of the total NMDA-R current is carried by Ca ions (Garaschuk et al., 1996; Schneggenburger et al., 1993), this drop in Ca permeability would be difficult to detect in synaptic currents. The selective regulation of NMDA-R Ca signals may thus explain why this form of postsynaptic $GABA_B$-R modulation has not been previously observed. Finally, these results also suggest that the effect of $GABA_B$-R activation on extracellularly evoked AMPA-R and NMDA-R EPSCs mostly reflects presynaptic modulation of glutamate release and not postsynaptic modulation of these receptors.

Presynaptic regulation

Previous experiments on $GABA_B$-R modulation of synaptic transmission have primarily focused on suppression of release, which occurs at many synapses throughout the brain. Two-photon optical quantal analysis allowed us to directly measure successful transmission and assess the impact of $GABA_B$-Rs on release. This approach has previously been used to examine presynaptic influences of other modulators in different brain regions (Higley et al., 2009; Oertner et al., 2002). In our experiments, $GABA_B$-R activation causes a strong drop in release probability, indicating direct modulation of presynaptic transmission. However, $GABA_B$-R activation also leads to a decrease in synaptic potency, which could result from either pre- or post-synaptic regulation.

Many synapses undergo multivesicular release, which can lead to graded synaptic responses (Foster et al., 2002; Wadiche and Jahr, 2001). Presynaptic inhibition reduces the release probability, causing less multivesicular release, lower synaptic glutamate concentration, and smaller postsynaptic responses. At other synapses, this kind of inhibition alone can explain the

modulation of NMDA-R Ca signals (Higley et al., 2009; Oertner et al., 2002). In our experiments using 2 mM Ca and GDP-βS to block postsynaptic modulation, $GABA_B$-R activation reduced both the release probability and synaptic potency, consistent with reduced multivesicular release. In support of this conclusion, in our experiments using 1 mM Ca and GDP-βS, in which the release probability was already reduced, $GABA_B$-R activation reduced only the release probability. These results suggest that reduced multivesicular release can contribute to changes in synaptic potency at this synapse, presumably by lowering the synaptic glutamate concentration detected by NMDA-Rs.

Relative contributions

What is the relative contribution of pre- and post-synaptic $GABA_B$-Rs to the modulation of NMDA-R Ca signals? The answer may depend on the level of ongoing synaptic activity. For example, presynaptic effects may be prominent when the probability of release is high and multivesicular release is prominent. When release probability falls, due to short-term plasticity or the influences of other modulators, these presynaptic effects may play a smaller role. Similarly, under physiological conditions, in which Ca in the cortex is closer to 1 mM (Somjen, 2004), multivesicular release may be less prominent, and presynaptic effects may be less important. In contrast, postsynaptic modulation may always influence activated NMDA-Rs, and therefore consistently inhibit Ca signals in dendritic spines.

Our experiments indicate differential sensitivity of pre- and post-synaptic modulation to $GABA_B$-R activation. For example, we observed prominent presynaptic modulation with 1 μM baclofen and complete inhibition at 5 μM baclofen. In contrast, we observed only moderate postsynaptic modulation with 1 μM baclofen but prominent suppression at 5 μM baclofen. There are several factors that could produce this difference, including: 1) unique types of $GABA_B$-Rs present at pre- and post-synaptic locations (Perez-Garci et al., 2006; Vigot et al., 2006), 2) distinct intracellular pathways mediating pre- and post-synaptic modulation (Bettler et al., 2004; Mott and Lewis, 1994), and 3) amplification of presynaptic inhibition by the power law for neurotransmitter release (Dittman and Regehr, 1996). In future experiments, it will be interesting to test the related hypothesis that presynaptic modulation may also be more sensitive to GABA, with postsynaptic modulation requiring greater levels of inhibitory activity.

Functional consequences

Throughout the brain, $GABA_B$-R activation controls many aspects of excitatory synaptic transmission. Presynaptic $GABA_B$-Rs regulate the probability of neurotransmitter release and shape the synaptic glutamate signal. Postsynaptic $GABA_B$-Rs activate inwardly rectifying K channels to generate a shunting conductance or hyperpolarization. Our results demonstrate for the first time that $GABA_B$-Rs also directly modulate postsynaptic NMDA-R Ca signals in spines. Thus, in addition to modulating the electrical properties of neurons, $GABA_B$-Rs also have the capability to influence the biochemical signaling cascades generated at synapses. This is a fundamentally new mechanism by which GABA signaling helps to control communication between neurons in the brain.

The modulation of spine Ca signals has widespread implications for the physiology, development and disease of neurons and their circuits. During synaptic activity, NMDA-R Ca signals reach high concentrations to activate signaling pathways that trigger diverse neuronal responses (Berridge, 1998; Kennedy, 2000; Zucker, 1999). These Ca signals are particularly important for synaptic plasticity, including both long-term potentiation and depression (Collingridge et al., 1983; Cummings et al., 1996; Dudek and Bear, 1992). They also influence dendrite and spine excitability by participating in local feedback loops with other Ca-sensitive ion channels (Bloodgood and Sabatini, 2007). In addition to these physiological effects, NMDA-R Ca signals play critical roles in morphogenesis (Engert and Bonhoeffer, 1999;

Maletic-Savatic et al., 1999), gene expression (Bito et al., 1997) and excitotoxicity (Vanhoutte and Bading, 2003). By regulating NMDA-R Ca signals in spines, post-synaptic $GABA_B$-R have the capacity to influence these and other essential aspects of Ca-dependent neuronal function.

Experimental Procedures

Preparation

Recordings were made from layer 2/3 pyramidal neurons in the medial prefrontal cortex (PFC) of acute slices from P21 - P28 C57/BL6 mice. Briefly, mice were anesthetized with a lethal dose of ketamine / xylazine and perfused intracardially with ice-cold external solution containing (in mM): 65 sucrose, 75 NaCl, 25 $NaHCO_3$, 1.25 NaH_2PO_4, 25 glucose, 2.5 KCl, 1 $CaCl_2$, 5 $MgCl_2$, 0.4 Na ascorbate, 3 Na pyruvate, bubbled with 95% O_2 / 5% CO_2. Coronal slices (300 μm thick) were cut in ice-cold external solution and transferred to ACSF containing (in mM): 119 NaCl, 25 $NaHCO_3$, 1.25 NaH_2PO_4, 25 glucose, 2.5 KCl, 2 $CaCl_2$, 1 $MgCl_2$, 0.4 Na-ascorbate, 3 Na-pyruvate, bubbled with 95% O_2 / 5% CO_2. After 30 minutes in ACSF at 35 °C, slices were stored for approximately 30 minutes at 24 °C, after which experiments were conducted at 33 - 34 °C. For experiments in 0 mM extracellular Mg, slices were incubated in ACSF containing NBQX, 2 mM Ca and 0 mM Mg for one hour before recording.

In all experiments, 10 μM D-serine and 10 μM gabazine were present in the ACSF, to prevent NMDA-R desensitization and block $GABA_A$-Rs, respectively. In some experiments, one or more of the following drugs were added to the ACSF (in μM): 10 NBQX, 10 (R)-CPP, 1 TTX, 1 ω-conotoxin-MVIIC, 0.3 SNX-482, 20 nimodipine, 10 mibefradil, 10 H89, 50 forskolin, 30 CPA, 1 or 5 (R)-baclofen. The cocktail of voltage-sensitive Ca channel (VSCC) blockers consisted of ω-conotoxin-MVIIC, SNX-482, nimodipine and mibefradil. This cocktail blocks Ca signals evoked by back-propagating action potentials (Figure S1), which are readily observed in the dendrites of these neurons (Larkum et al., 2007). In extracellular stimulation experiments (Figure 1), (R)-CPP or NBQX was added to the bath to isolate AMPA-R or NMDA-R EPSCs, respectively.All chemicals were from Sigma or Tocris, with the exception of SNX-482 and ω-conotoxin-MVIIC (Peptides International, Inc.) and PKC inhibitor peptide (19-36) (PKC-I) (Calbiochem).

Physiology recordings

Whole-cell recordings were obtained from layer 2/3 pyramidal neurons identified with IR-DIC at 200 - 300 μm from the pial surface. Borosilicate recording pipettes (2 - 5 MΩ) were filled with 1 of 2 internal solutions. Current-clamp recordings used (in mM): 135 K-gluconate, 7 KCl, 10 HEPES, 10 Na-phosphocreatine, 4 Mg_2-ATP, 0.4 NaGTP, 290-295 mOsm, pH 7.35 with KOH. Voltage-clamp recordings used (in mM): 135 Cs-gluconate, 10 HEPES, 10 Na-phosphocreatine, 4 Mg_2-ATP, 0.4 NaGTP, 290-295 mOsm, pH 7.35 with CsOH. Solutions also contained Fluo-5F (1000 μM for voltage-clamp, 200 μM for current-clamp) to monitor Ca levels and Alexa Fluor-594 (20 μM) to image neuronal morphology. Neurons were filled via the patch electrode for at least 15 - 20 min before imaging. Dye concentrations were chosen to ensure that Ca signals were in the linear range of the indicators (Yasuda et al., 2004). In some experiments, one of the following drugs were added to the internal solution (in mM): 3 Guanosine-5′-[β-thio]diphosphate trilithium salt (GDP-βS), 0.1 PKA inhibitor fragment (6-22) (PKI), or 0.1 PKC inhibitor peptide (19-36) (PKC-I).

Recordings were made using a Multiclamp 700B amplifier, filtered at 5 kHz for current-clamp recordings and 2 kHz for voltage-clamp recordings, and sampled at 10 kHz. Action potentials were triggered with brief (2 ms) current injections (1200 - 2000 pA) through the recording pipette. Excitatory input fibers were stimulated with a theta-glass bipolar electrode (tip

diameter 1 - 4 μm) filled with the extracellular ACSF, using brief (0.2 ms) and small (5 - 20 μA) current injections. The electrode was placed approximately 1 - 5 μm from the spine of interest, and the spatial resolution of this approach was found to be high.

Two-photon microscopy

Intracellular Ca imaging and glutamate uncaging was accomplished with a custom microscope that combines two-photon laser scanning microscopy (2PLSM) and two-photon laser uncaging (2PLU), as previously described (Carter and Sabatini, 2004; Carter et al., 2007). For all experiments, proximal spines in the basal dendrites within a radial distance of 75 μm from the soma were chosen to reduce voltage-clamp errors.

For 2PLSM, 810 nm light was used to excite Fluo-5F (green) and Alexa Fluor-594 (red), in order to monitor Ca signals and spine morphology, respectively. Reference frame scans were taken between each acquisition in order to correct for small spatial drift of the preparation over time. To measure Ca signals, green and red fluorescence were collected during 500 Hz line scans across a dendrite-spine or spine-spine pair. Ca signals were quantified as changes in green fluorescence to red fluorescence (ΔG/R), normalized to the maximal green fluorescence to red fluorescence (G_{sat}/R), giving $\Delta G/G_{sat}$ (Bloodgood and Sabatini, 2007). The value of G_{sat}/R was measured after each recording using a thin-walled pipette, containing a saturating concentration of Ca (Yasuda et al., 2004), which was positioned directly above the recorded cell and used at the same recording temperature (33 - 34 °C).

For two-photon optical quantal analysis, cells were voltage-clamped at +10 mV to relieve magnesium block and to inactivate VSCCs (Oertner et al., 2002). Experiments were performed in the presence of (D)-serine, gabazine, and NBQX. Line-scans with electrical stimulation were interleaved with line-scans with no stimulation. Line-scans were acquired every 15 s for a total of 40 stimulation trials (20 baseline, 20 drug). Baclofen was washed-in for 5 minutes before the drug trials. To classify successful trials, the threshold for each spine was set to two standard deviations of the signal in the line-scans with no stimulation. To confirm that small amounts of drift did not result in losing the axon of interest, two stimuli (50 ms inter-stimulus interval) were occasionally given to confirm that the spine was activated. During normal (2 mM) Ca experiments, spines with Ca signals above the linear range of the indicator were excluded from analysis. During low (1 mM) Ca experiments, 4 out of 12 spines showed no synaptic responses after wash-in of 1 μM baclofen and were excluded from the analysis. In Figures 2 & 3, individual $\Delta G/G_{sat}$ trials are filtered for display purposes.

For 2PLU, MNI-glutamate was bath applied at 2.5 mM in 6 - 12 ml of ACSF. All experiments were performed in the presence of (D)-serine, gabazine, and TTX. (R)-CPP or NBQX was added to isolate AMPA-R or NMDA-R uEPSCs, respectively. Experiments at −70 mV, 0 mM Mg and −20 mV, 1 mM Mg were performed in the presence of the VSCC blockers. Glutamate uncaging was achieved using a 1 ms pulse of 725 nm light. The uncaging location was chosen at 0.5 μm from the spine head. At this distance, photobleaching and photodamage are minimal but uEPSCs and Ca signals can be readily obtained (Carter et al., 2007). The laser intensity was chosen to mimic the amplitude of spontaneous AMPA-R EPSCs or extracellularly evoked NMDA-R Ca signals. Similar to experiments using two-photon optical quantal analysis, line-scans were acquired every 15 s for a total of 40 stimulation trials (20 baseline, 20 drug). Baclofen was washed-in for 5 minutes before the drug trials. Baseline fluorescence was monitored and recordings were discarded if an increase was detected, which would indicate photodamage.

Data acquisition and analysis

Image and physiology data were acquired using National Instruments boards and custom software written in MATLAB (Mathworks). Off-line analysis was performed using custom routines written in Igor Pro (Wavemetrics). The amplitudes of EPSCs and uEPSCs are averages over a 1 ms time window around the peak. The amplitudes of NMDA-R Ca signals are averages over a 150 ms time period, starting 50 ms after the stimulus. In Figures 2, 5 & 8, images of spines and dendrites were treated with a 1.5-pixel-radius Gaussian filter for display purposes.

Summary data are reported as median ± standard error. The standard error was calculated as the standard deviation of the medians calculated from 10,000 bootstrapped samples from the data. Electrophysiological and imaging data are shown as the arithmetic mean ± standard error from multiple trials of the experiment. There were occasionally small differences between the mean and median within a group, which explains some discrepancies between average traces in figures and medians reported in the text. Most summary data is in box plot form, showing the median, interquartile range, 10 - 90% range (whiskers), and including the data from individual experiments (open circles). Significance was defined as $P < 0.05$ (*) and determined using the non-parametric Wilcoxon-Mann-Whitney two-sample rank test or the Wilcoxon signed rank test for paired data (when appropriate), both of which make no assumptions about the data distribution.

Supplementary Material

Refer to Web version on PubMed Central for supplementary material.

Acknowledgments

We thank members of the Carter lab, Michael Beierlein, Alex Reyes and Eric Klann for helpful discussions and comments on the manuscript. This work was supported by NARSAD, Klingenstein Fund, Whitehall Foundation and NIH 1R01MH085974-01A1.

References

Alger BE. Characteristics of a slow hyperpolarizing synaptic potential in rat hippocampal pyramidal cells in vitro. Journal of Neurophysiology 1984;52:892–910. [PubMed: 6096520]

Beaulieu C, Somogyi P. Targets and Quantitative Distribution of GABAergic Synapses in the Visual Cortex of the Cat. Eur J Neurosci 1990;2:296–303. [PubMed: 12106036]

Benardo LS. Separate activation of fast and slow inhibitory postsynaptic potentials in rat neocortex in vitro. The Journal of Physiology 1994;476:203–215. [PubMed: 7913968]

Berridge MJ. Neuronal calcium signaling. Neuron 1998;21:13–26. [PubMed: 9697848]

Bettler B, Kaupmann K, Bowery N. GABAB receptors: drugs meet clones. Curr Opin Neurobiol 1998;8:345–350. [PubMed: 9687348]

Bettler B, Kaupmann K, Mosbacher J, Gassmann M. Molecular structure and physiological functions of GABA(B) receptors. Physiological Reviews 2004;84:835–867. [PubMed: 15269338]

Bito H, Deisseroth K, Tsien R. Ca2+-dependent regulation in neuronal gene expression. Curr Opin Neurobiol 1997;7:419–429. [PubMed: 9232807]

Blank T, Nijholt I, Teichert U, Kügler H, Behrsing H, Fienberg A, Greengard P, Spiess J. The phosphoprotein DARPP-32 mediates cAMP-dependent potentiation of striatal N-methyl-D-aspartate responses. Proc Natl Acad Sci USA 1997;94:14859–14864. [PubMed: 9405704]

Bloodgood BL, Sabatini BL. Nonlinear regulation of unitary synaptic signals by CaV(2.3) voltage-sensitive calcium channels located in dendritic spines. Neuron 2007;53:249–260. [PubMed: 17224406]

Bowery NG, Bettler B, Froestl W, Gallagher JP, Marshall F, Raiteri M, Bonner TI, Enna SJ. International Union of Pharmacology. XXXIII. Mammalian gamma-aminobutyric acid(B) receptors: structure and function. Pharmacol Rev 2002;54:247–264. [PubMed: 12037141]

Caddick SJ, Hosford DA. The role of GABAB mechanisms in animal models of absence seizures. Mol Neurobiol 1996;13:23–32. [PubMed: 8892334]

Carter AG, Sabatini BL. State-dependent calcium signaling in dendritic spines of striatal medium spiny neurons. Neuron 2004;44:483–493. [PubMed: 15504328]

Carter AG, Soler-Llavina GJ, Sabatini BL. Timing and location of synaptic inputs determine modes of subthreshold integration in striatal medium spiny neurons. J Neurosci 2007;27:8967–8977. [PubMed: 17699678]

Collingridge GL, Kehl SJ, McLennan H. Excitatory amino acids in synaptic transmission in the Schaffer collateral-commissural pathway of the rat hippocampus. The Journal of Physiology 1983;334:33–46. [PubMed: 6306230]

Cummings JA, Mulkey RM, Nicoll RA, Malenka RC. Ca2+ signaling requirements for long-term depression in the hippocampus. Neuron 1996;16:825–833. [PubMed: 8608000]

Dittman JS, Regehr WG. Contributions of calcium-dependent and calcium-independent mechanisms to presynaptic inhibition at a cerebellar synapse. J Neurosci 1996;16:1623–1633. [PubMed: 8774431]

Dittman JS, Regehr WG. Mechanism and kinetics of heterosynaptic depression at a cerebellar synapse. J Neurosci 1997;17:9048–9059. [PubMed: 9364051]

Doupnik CA, Davidson N, Lester HA. The inward rectifier potassium channel family. Curr Opin Neurobiol 1995;5:268–277. [PubMed: 7580148]

Dudek SM, Bear MF. Homosynaptic long-term depression in area CA1 of hippocampus and effects of N-methyl-D-aspartate receptor blockade. Proc Natl Acad Sci USA 1992;89:4363–4367. [PubMed: 1350090]

Dutar P, Nicoll R. A physiological role for GABAB receptors in the central nervous system. Nature 1988;332:156–158. [PubMed: 2831457]

Engert F, Bonhoeffer T. Dendritic spine changes associated with hippocampal long-term synaptic plasticity. Nature 1999;399:66–70. [PubMed: 10331391]

Foster KA, Kreitzer AC, Regehr WG. Interaction of postsynaptic receptor saturation with presynaptic mechanisms produces a reliable synapse. Neuron 2002;36:1115–1126. [PubMed: 12495626]

Gähwiler BH, Brown DA. GABAB-receptor-activated K+ current in voltage-clamped CA3 pyramidal cells in hippocampal cultures. Proc Natl Acad Sci USA 1985;82:1558–1562. [PubMed: 2983351]

Garaschuk O, Schneggenburger R, Schirra C, Tempia F, Konnerth A. Fractional Ca2+ currents through somatic and dendritic glutamate receptor channels of rat hippocampal CA1 pyramidal neurones. The Journal of Physiology 1996;491(Pt 3):757–772. [PubMed: 8815209]

Higley MJ, Soler-Llavina GJ, Sabatini BL. Cholinergic modulation of multivesicular release regulates striatal synaptic potency and integration. Nat. Neurosci 2009:1–10. [PubMed: 19107139]

Hollmann M, Heinemann S. Cloned glutamate receptors. Annu Rev Neurosci 1994;17:31–108. [PubMed: 8210177]

Isaacson JS, Solís JM, Nicoll RA. Local and diffuse synaptic actions of GABA in the hippocampus. Neuron 1993;10:165–175. [PubMed: 7679913]

Kaupmann K, Malitschek B, Schuler V, Heid J, Froestl W, Beck P, Mosbacher J, Bischoff S, Kulik A, Shigemoto R, et al. GABA(B)-receptor subtypes assemble into functional heteromeric complexes. Nature 1998;396:683–687. [PubMed: 9872317]

Kennedy MB. Signal-processing machines at the postsynaptic density. Science 2000;290:750–754. [PubMed: 11052931]

Kovalchuk Y, Eilers J, Lisman J, Konnerth A. NMDA receptor-mediated subthreshold Ca(2+) signals in spines of hippocampal neurons. J Neurosci 2000;20:1791–1799. [PubMed: 10684880]

Kulik A, Vida I, Fukazawa Y, Guetg N, Kasugai Y, Marker CL, Rigato F, Bettler B, Wickman K, Frotscher M, Shigemoto R. Compartment-dependent colocalization of Kir3.2-containing K+ channels and GABAB receptors in hippocampal pyramidal cells. J Neurosci 2006;26:4289–4297. [PubMed: 16624949]

Larkman A. Dendritic morphology of pyramidal neurones of the visual cortex of the rat: III. Spine distributions. J Comp Neurol 1991;306:332–343. [PubMed: 1711059]

Larkum ME, Waters J, Sakmann B, Helmchen F. Dendritic Spikes in Apical Dendrites of Neocortical Layer 2/3 Pyramidal Neurons. Journal of Neuroscience 2007;27:8999–9008. [PubMed: 17715337]

Leonard AS, Hell JW. Cyclic AMP-dependent protein kinase and protein kinase C phosphorylate N-methyl-D-aspartate receptors at different sites. J Biol Chem 1997;272:12107–12115. [PubMed: 9115280]

Lüscher C, Jan LY, Stoffel M, Malenka RC, Nicoll RA. G protein-coupled inwardly rectifying K+ channels (GIRKs) mediate postsynaptic but not presynaptic transmitter actions in hippocampal neurons. Neuron 1997;19:687–695. [PubMed: 9331358]

Mainen ZF, Malinow R, Svoboda K. Synaptic calcium transients in single spines indicate that NMDA receptors are not saturated. Nature 1999;399:151–155. [PubMed: 10335844]

Maletic-Savatic M, Malinow R, Svoboda K. Rapid dendritic morphogenesis in CA1 hippocampal dendrites induced by synaptic activity. Science 1999;283:1923–1927. [PubMed: 10082466]

Matsuzaki M, Ellis-Davies G, Nemoto T, Miyashita Y, Iino M, Kasai H. Dendritic spine geometry is critical for AMPA receptor expression in hippocampal CA1 pyramidal neurons. Nat Neurosci 2001;4:1086–1092. [PubMed: 11687814]

Mintz I, Bean B. GABAB receptor inhibition of P-type Ca2+ channels in central neurons. Neuron 1993;10:889–898. [PubMed: 8388225]

Misgeld U, Bijak M, Jarolimek W. A physiological role for GABAB receptors and the effects of baclofen in the mammalian central nervous system. Prog Neurobiol 1995;46:423–462. [PubMed: 8532848]

Morrisett R, Mott D, Lewis D, Swartzwelder H, Wilson W. GABAB-receptor-mediated inhibition of the N-methyl-D-aspartate component of synaptic transmission in the rat hippocampus. J Neurosci 1991;11:203–209. [PubMed: 1846009]

Mott DD, Lewis DA. The pharmacology and function of central GABAB receptors. Int Rev Neurobiol 1994;36:97–223. [PubMed: 7822122]

Newberry NR, Nicoll RA. A bicuculline-resistant inhibitory post-synaptic potential in rat hippocampal pyramidal cells in vitro. The Journal of Physiology 1984;348:239–254. [PubMed: 6716285]

Newberry NR, Nicoll RA. Comparison of the action of baclofen with gamma-aminobutyric acid on rat hippocampal pyramidal cells in vitro. The Journal of Physiology 1985;360:161–185. [PubMed: 3989713]

Oertner T, Sabatini B, Nimchinsky E, Svoboda K. Facilitation at single synapses probed with optical quantal analysis. Nat Neurosci 2002;5:657–664. [PubMed: 12055631]

Otmakhova N, Lisman J. Contribution of Ih and GABAB to synaptically induced afterhyperpolarizations in CA1: a brake on the NMDA response. J Neurophysiol 2004;92:2027–2039. [PubMed: 15163674]

Perez-Garci E, Gassmann M, Bettler B, Larkum M. The GABAB1b isoform mediates long-lasting inhibition of dendritic Ca2+ spikes in layer 5 somatosensory pyramidal neurons. Neuron 2006;50:603–616. [PubMed: 16701210]

Pfrieger F, Gottmann K, Lux H. Kinetics of GABAB receptor-mediated inhibition of calcium currents and excitatory synaptic transmission in hippocampal neurons in vitro. Neuron 1994;12:97–107. [PubMed: 8292363]

Raman IM, Tong G, Jahr CE. Beta-adrenergic regulation of synaptic NMDA receptors by cAMP-dependent protein kinase. Neuron 1996;16:415–421. [PubMed: 8789956]

Sabatini BL, Svoboda K. Analysis of calcium channels in single spines using optical fluctuation analysis. Nature 2000;408:589–593. [PubMed: 11117746]

Sakaba T, Neher E. Direct modulation of synaptic vesicle priming by GABAB receptor activation at a glutamatergic synapse. Nature 2003;424:775–778. [PubMed: 12917685]

Scanziani M, Capogna M, Gähwiler BH, Thompson SM. Presynaptic inhibition of miniature excitatory synaptic currents by baclofen and adenosine in the hippocampus. Neuron 1992;9:919–927. [PubMed: 1358131]

Schneggenburger R, Zhou Z, Konnerth A, Neher E. Fractional contribution of calcium to the cation current through glutamate receptor channels. Neuron 1993;11:133–143. [PubMed: 7687849]

Scholz KP, Miller RJ. GABAB receptor-mediated inhibition of Ca2+ currents and synaptic transmission in cultured rat hippocampal neurones. The Journal of Physiology 1991;444:669–686. [PubMed: 1668352]

Sivilotti L, Nistri A. GABA receptor mechanisms in the central nervous system. Prog Neurobiol 1991;36:35–92. [PubMed: 1847747]

Skeberdis VA, Chevaleyre V, Lau CG, Goldberg JH, Pettit DL, Suadicani SO, Lin Y, Bennett MVL, Yuste R, Castillo PE, Zukin RS. Protein kinase A regulates calcium permeability of NMDA receptors. Nat. Neurosci 2006;9:501–510. [PubMed: 16531999]

Sobczyk A, Svoboda K. Activity-dependent plasticity of the NMDA-receptor fractional Ca2+ current. Neuron 2007;53:17–24. [PubMed: 17196527]

Sodickson D, Bean B. GABAB receptor-activated inwardly rectifying potassium current in dissociated hippocampal CA3 neurons. J Neurosci 1996;16:6374–6385. [PubMed: 8815916]

Somjen, G., editor. Ions in the Brain: Normal Function, Seizures, and Stroke. Oxford Univ. Press; Oxford, UK: 2004.

Takahashi T, Kajikawa Y, Tsujimoto T. G-Protein-coupled modulation of presynaptic calcium currents and transmitter release by a GABAB receptor. J Neurosci 1998;18:3138–3146. [PubMed: 9547222]

Tingley WG, Ehlers MD, Kameyama K, Doherty C, Ptak JB, Riley CT, Huganir RL. Characterization of protein kinase A and protein kinase C phosphorylation of the N-methyl-D-aspartate receptor NR1 subunit using phosphorylation site-specific antibodies. J Biol Chem 1997;272:5157–5166. [PubMed: 9030583]

Vanhoutte P, Bading H. Opposing roles of synaptic and extrasynaptic NMDA receptors in neuronal calcium signalling and BDNF gene regulation. Curr Opin Neurobiol 2003;13:366–371. [PubMed: 12850222]

Vigot R, Barbieri S, Bräuner-Osborne H, Turecek R, Shigemoto R, Zhang Y, Luján R, Jacobson LH, Biermann B, Fritschy J, et al. Differential compartmentalization and distinct functions of GABAB receptor variants. Neuron 2006;50:589–601. [PubMed: 16701209]

Wadiche JI, Jahr CE. Multivesicular release at climbing fiber-Purkinje cell synapses. Neuron 2001;32:301–313. [PubMed: 11683999]

Wang LY, Orser BA, Brautigan DL, MacDonald JF. Regulation of NMDA receptors in cultured hippocampal neurons by protein phosphatases 1 and 2A. Nature 1994;369:230–232. [PubMed: 8183343]

Westphal RS, Tavalin SJ, Lin JW, Alto NM, Fraser ID, Langeberg LK, Sheng M, Scott JD. Regulation of NMDA receptors by an associated phosphatase-kinase signaling complex. Science 1999;285:93–96. [PubMed: 10390370]

Wu LG, Saggau P. GABAB receptor-mediated presynaptic inhibition in guinea-pig hippocampus is caused by reduction of presynaptic Ca2+ influx. The Journal of Physiology 1995;485(Pt 3):649–657. [PubMed: 7562607]

Yasuda R, Nimchinsky E, Scheuss V, Pologruto T, Oertner T, Sabatini B, Svoboda K. Imaging calcium concentration dynamics in small neuronal compartments. Sci STKE 2004;2004:l5.

Zucker RS. Calcium- and activity-dependent synaptic plasticity. Curr Opin Neurobiol 1999;9:305–313. [PubMed: 10395573]

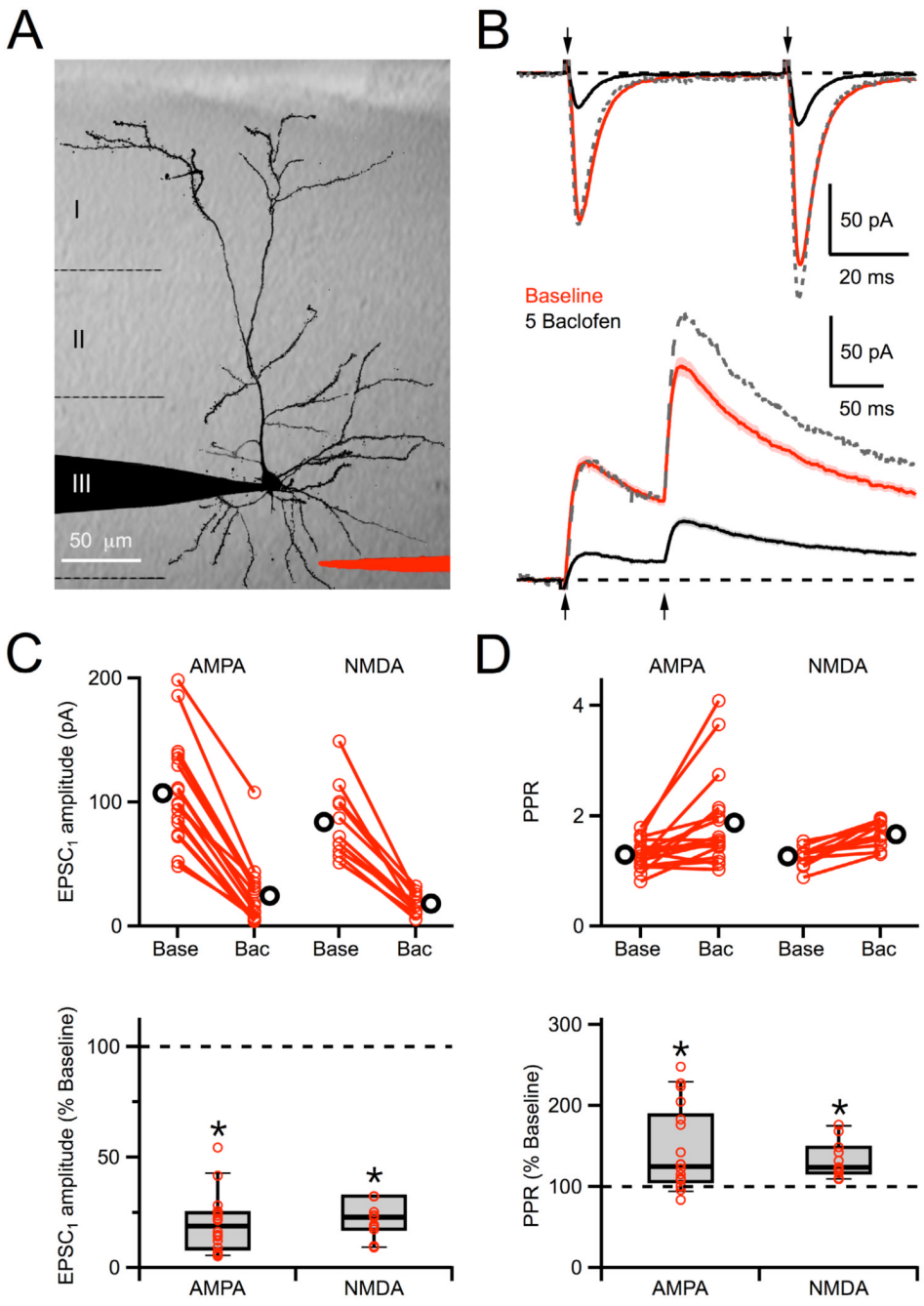

Figure 1. Modulation of synaptic transmission

A, 2PLSM image of a L2/3 pyramidal neuron, overlaid on an IR-DIC image of the cortical slice, showing recording (*black*) and theta-glass stimulating (*red*) pipettes. **B**, Paired-pulse stimulation (*arrows*, 50 ms inter-stimulus interval) evokes EPSCs mediated by AMPA-Rs at −70 mV (*top*) or NMDA-Rs at +40 mV (*bottom*) in baseline conditions (*red*) and following wash-in of 5 µM baclofen (*black*). The dotted grey line shows the baclofen traces scaled to the first EPSC amplitude in baseline conditions. Stimulus artifacts have been removed for clarity. **C**, Summary of the effect of 5 µM baclofen on the amplitude of the first AMPA-R and NMDA-R EPSCs. For non-normalized data (*top*), scatter plots show baseline conditions (*base*) and after wash-in of 5 µM baclofen (*bac*), where red circles connected by a line are individual

experiments before and after baclofen wash-in, and black circles are the averages. For normalized data (*bottom*), red circles indicate individual experiments and box plots show median, interquartile range, and 10 - 90% range. **D**, Summary of the effect of 5 μM baclofen on the paired-pulse ratio (PPR) of AMPA-R and NMDA-R EPSCs. Asterisks indicate significant ($P < 0.05$) difference from 100%.

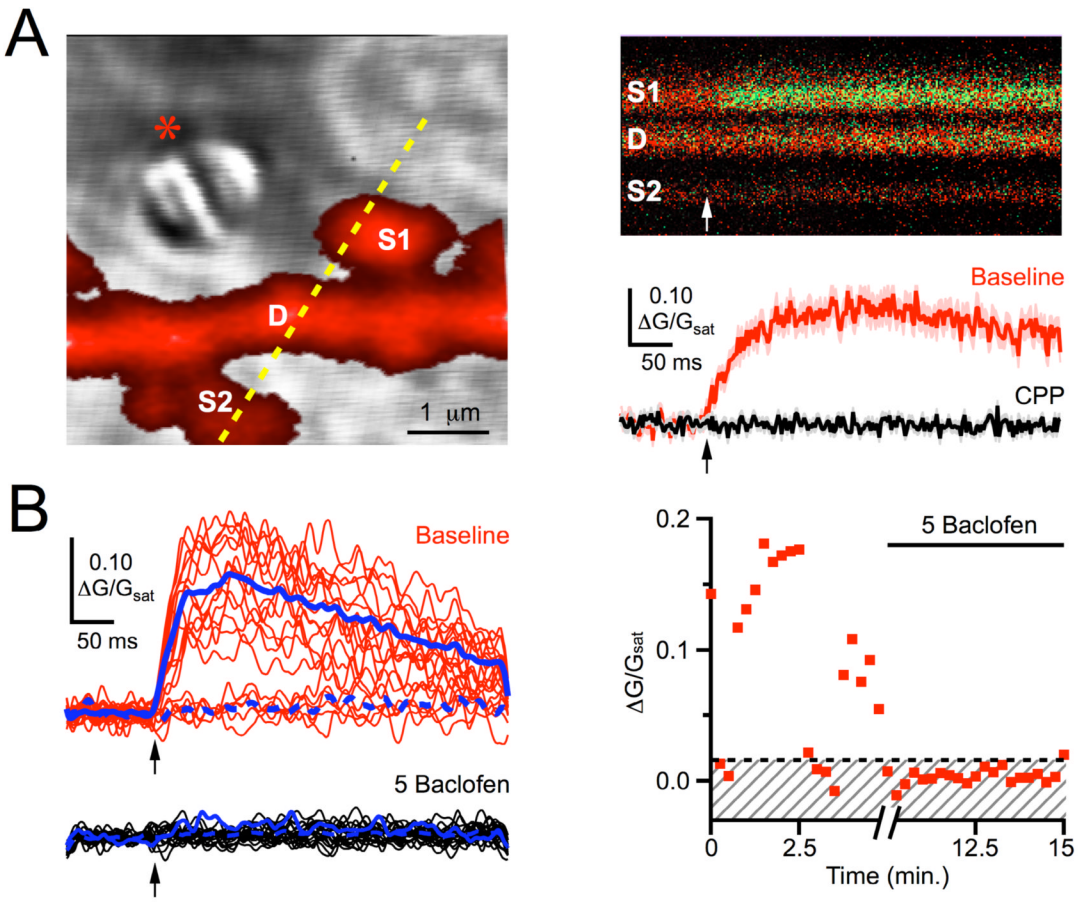

Figure 2. Modulation at single spines

A, *Left*, 2PLSM image of a dendrite (*D*) and two spines (S1 and S2), with dashed yellow line indicating line-scan position, overlaid on a LS-DIC image showing the theta-glass stimulating pipette (*star*). *Right*, During a 500 Hz line-scan through dendrite and spines, extracellular stimulation (*arrow*) evokes a green Ca transient only in S1 (*top*), quantified as $\Delta G/G_{sat}$ (*bottom*) in control conditions (*red*) and following wash-in of CPP (*black*). **B**, *Left*, Stochastic NMDA-R Ca signals in baseline conditions (*red*) and following wash-in of 5 μM baclofen (*black*), where solid and dashed blue lines indicate mean successes and failures, respectively. *Right*, Time-course of NMDA-R Ca signal amplitudes, where red dots are individual trials, the dashed black line is the calculated threshold, and the shaded region includes failures. For all time-courses, the break in the x-axis indicates the baclofen wash-in period (5 minutes) that occurs between 5 minutes of baseline acquisition and 5 minutes of baclofen acquisition.

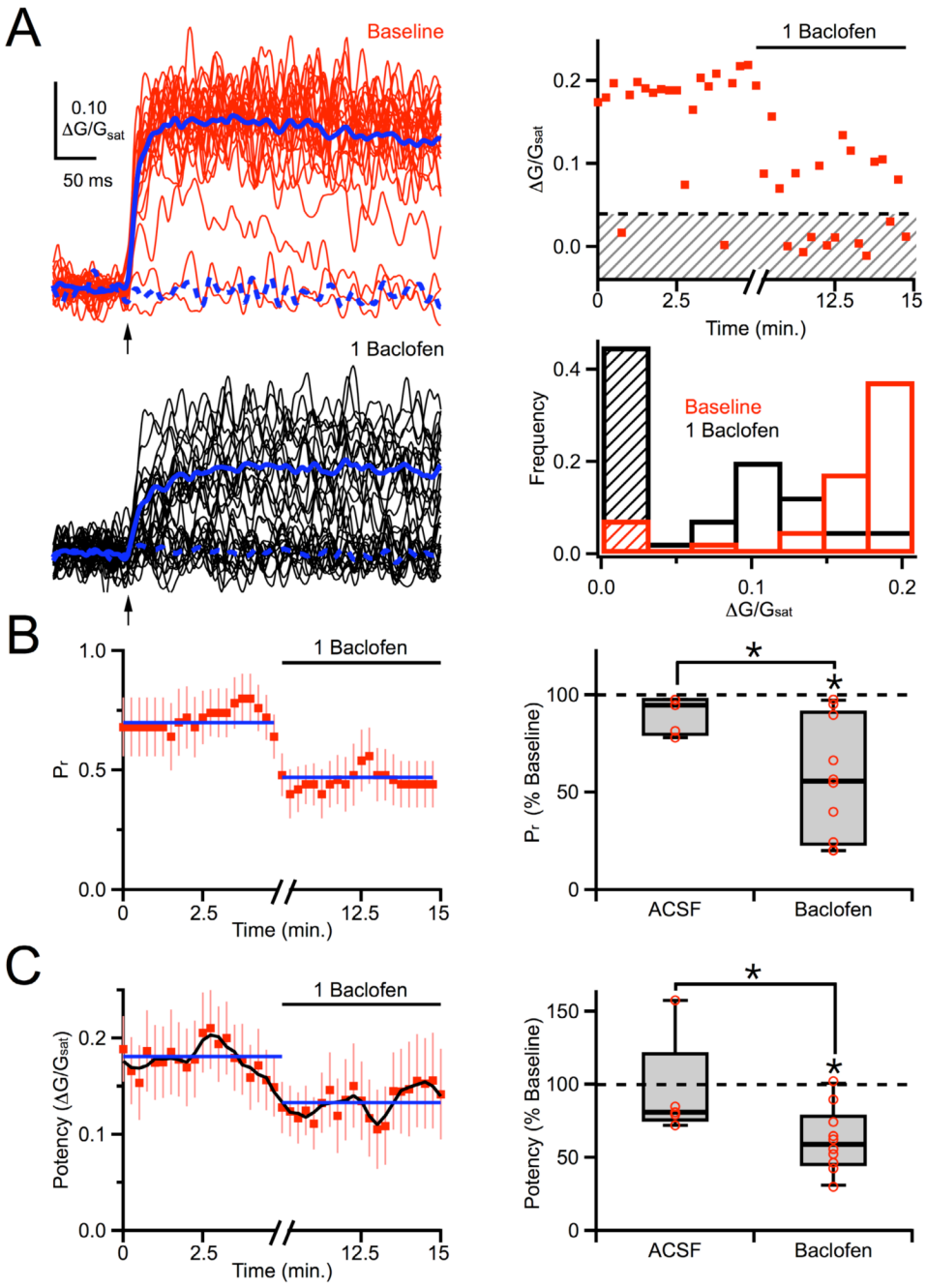

Figure 3. Two-photon optical quantal analysis

A, *Left*, Extracellularly-evoked NMDA-R Ca signals in baseline conditions (*red*) and following wash-in of 1 μM baclofen (*black*). *Right*, Time-course (*top*) of NMDA-R Ca signal amplitudes, where red dots are individual trials, the dashed black line is the calculated threshold, and the shaded region includes failures. Frequency histogram (*bottom*) of $\Delta G/G_{sat}$ signal amplitudes in baseline conditions (*red*) and following 1 μM baclofen (*black*), where the shaded regions include failures. **B**, *Left*, Average time-course of probability of release, calculated using a five point running window. Blue lines indicate average periods in baseline conditions and baclofen. *Right*, Summary of changes in probability of release following wash-in of baclofen or ACSF. **C**, *Left*, Average time-course of synaptic potency. The running average was calculated using

a five-point window and is shown as a black line. Blue lines indicate average periods in baseline conditions and baclofen. *Right*, Summary of changes in synaptic potency following wash-in of baclofen or ACSF. Asterisks indicate significant ($P < 0.05$) difference from 100% or between different conditions.

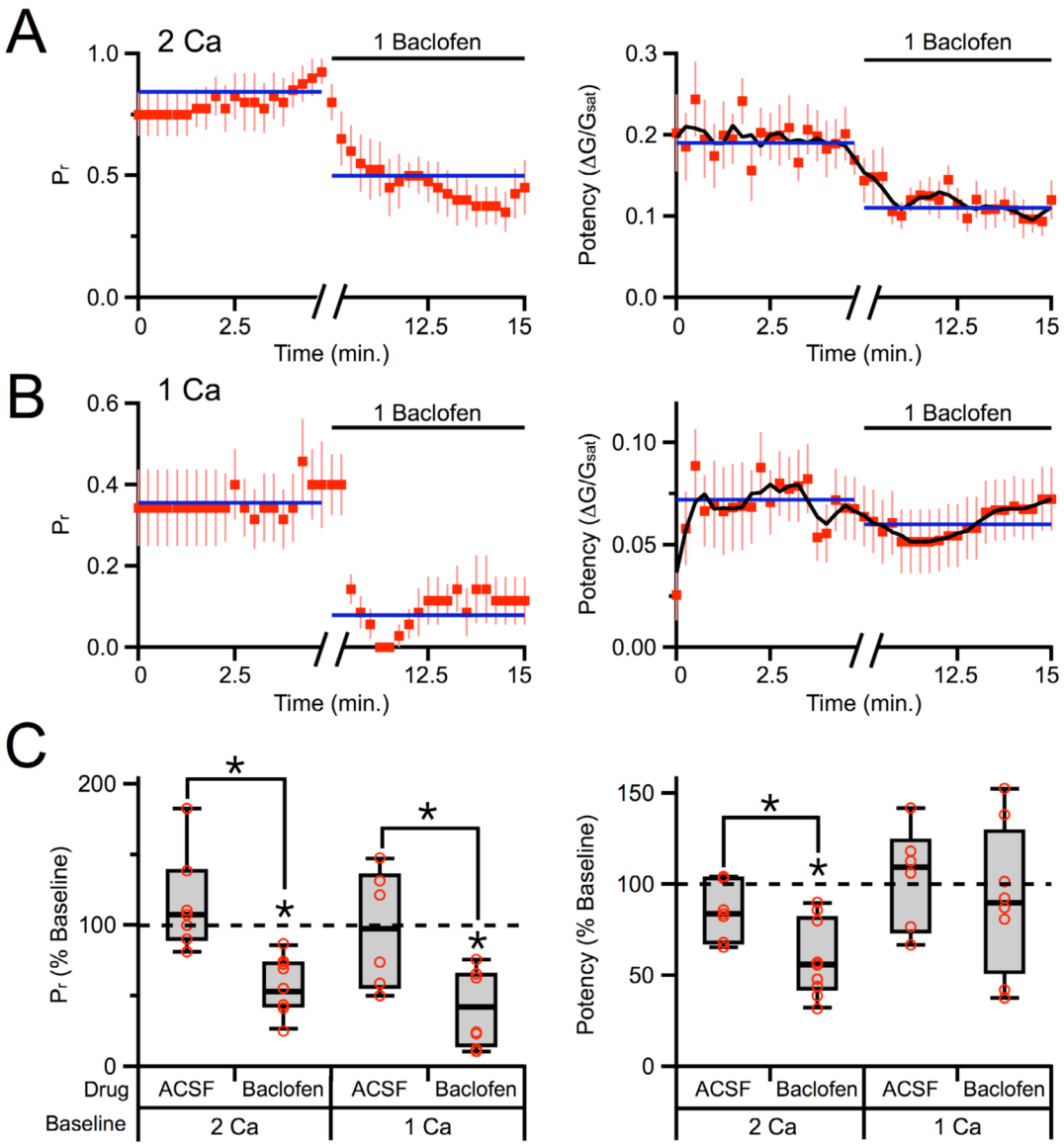

Figure 4. Contributions of multivesicular release

A, Average time-course of probability of release (*left*) and average time-course of synaptic potency (*right)* in 2 mM extracellular Ca and internal GDP-βS. The running average of the synaptic potency is shown as a black line. Blue lines indicate average periods in baseline conditions and baclofen. **B**, Equivalent results as in (A), measured in 1 mM extracellular Ca and internal GDP-βS. **C**, Summary of changes in probability of release (*left*) and synaptic potency (*right*) following wash-in of baclofen or ACSF in the different recording conditions. Asterisks indicate significant ($P < 0.05$) difference from 100% or between different conditions.

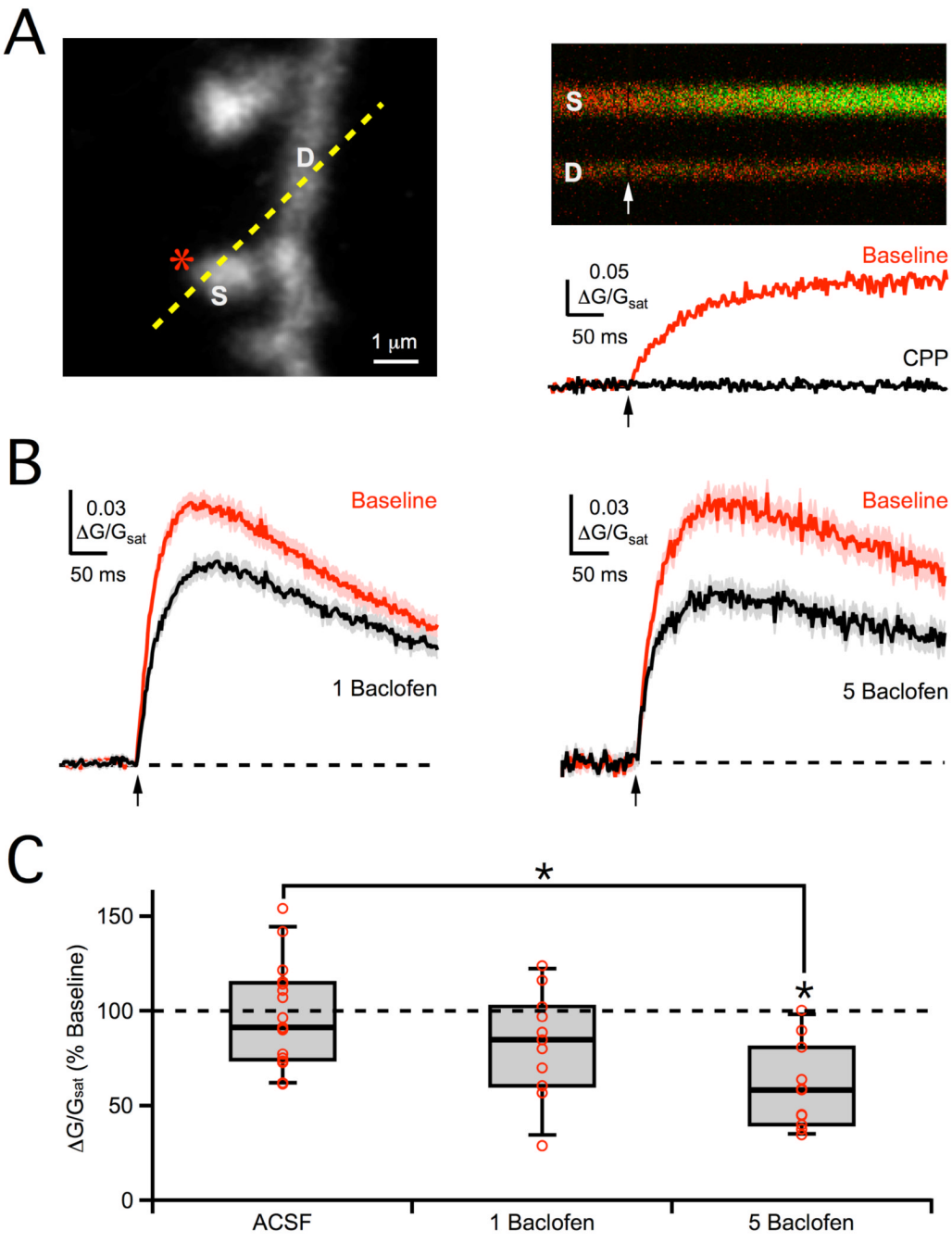

Figure 5. Postsynaptic modulation of NMDA-R Ca signals

A, *Left*, 2PLSM image of dendrite (D) and spine (S), showing uncaging location (*star*) and line-scan position (*dashed yellow line*). *Right*, Line-scan through dendrite and spine (*top*) during 2PLU (*arrows*), with change in green Ca transient quantified as $\Delta G/G_{sat}$ (*bottom*), in baseline conditions (*red*) and following wash-in of CPP (*black*). **B**, Average 2PLU-evoked NMDA-R Ca signals in baseline conditions (*red*) and following wash-in of 1 μM baclofen (*left*, *black*) or 5 μM baclofen (*right*, *black*). **C**, Summary of changes in NMDA-R Ca signal amplitude following wash-in of 5 μM baclofen, 1 μM baclofen or ACSF. Asterisks indicate significant ($P < 0.05$) difference from 100% or between different conditions.

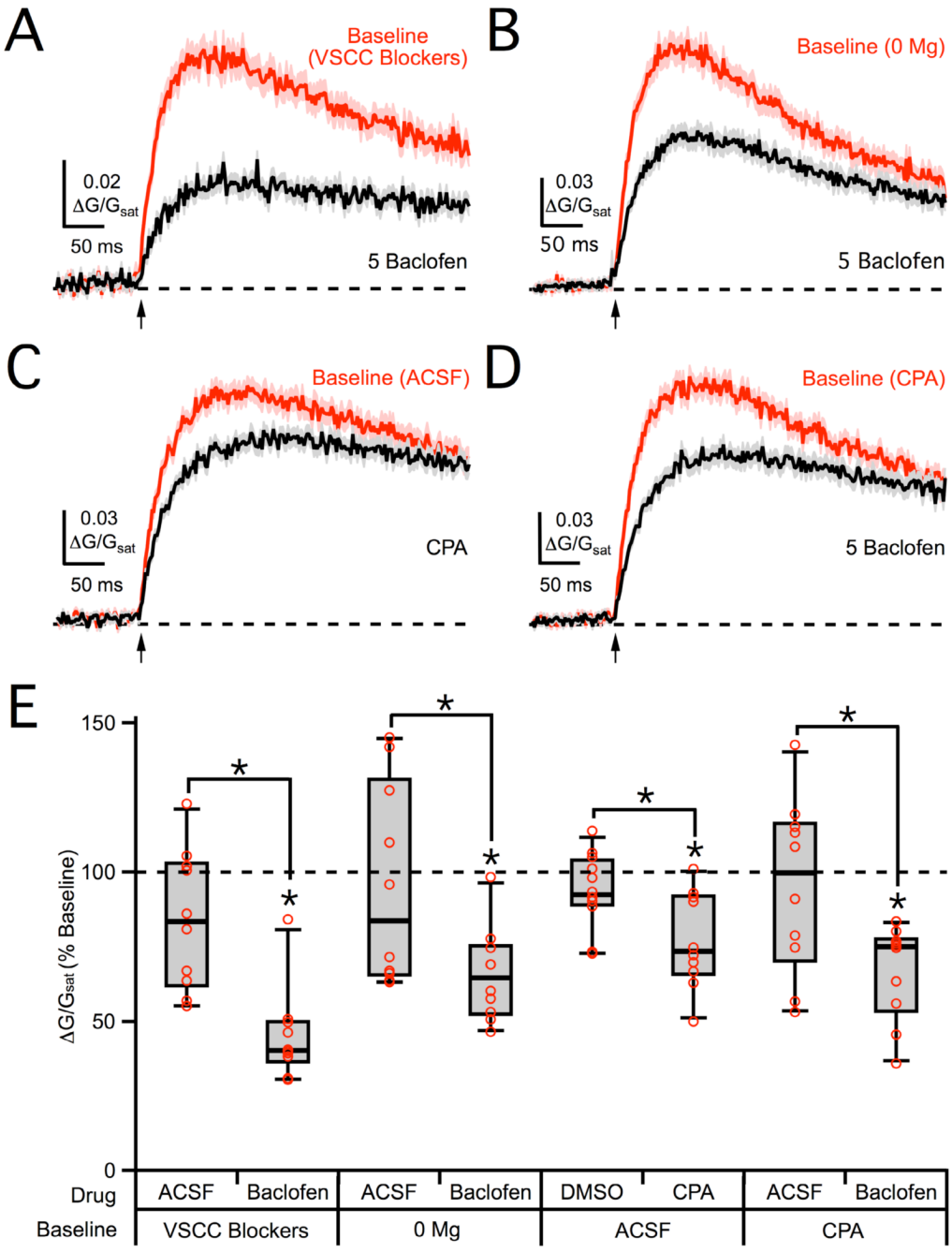

Figure 6. VSCCs, Mg block and internal Ca stores are not required for NMDA-R modulation

A, Average 2PLU-evoked NMDA-R Ca signals in VSCC blockers (*red*) and following wash-in of 5 μM baclofen (*black*). **B**, Average NMDA-R Ca signals in 0 mM Mg (*red*) and following wash-in of 5 μM baclofen (*black*). **C**, Average NMDA-R Ca signals in baseline ACSF (*red*) and following wash-in of CPA (*black*). **D**, Average NMDA-R Ca signals in CPA (*red*) and following wash-in of 5 μM baclofen (*black*). **E**, Summary of changes in NMDA-R Ca signal amplitude following wash-in of drugs or vehicle controls in the different recording conditions. Asterisks indicate significant ($P < 0.05$) difference from 100% or between different conditions. See also Figure S1.

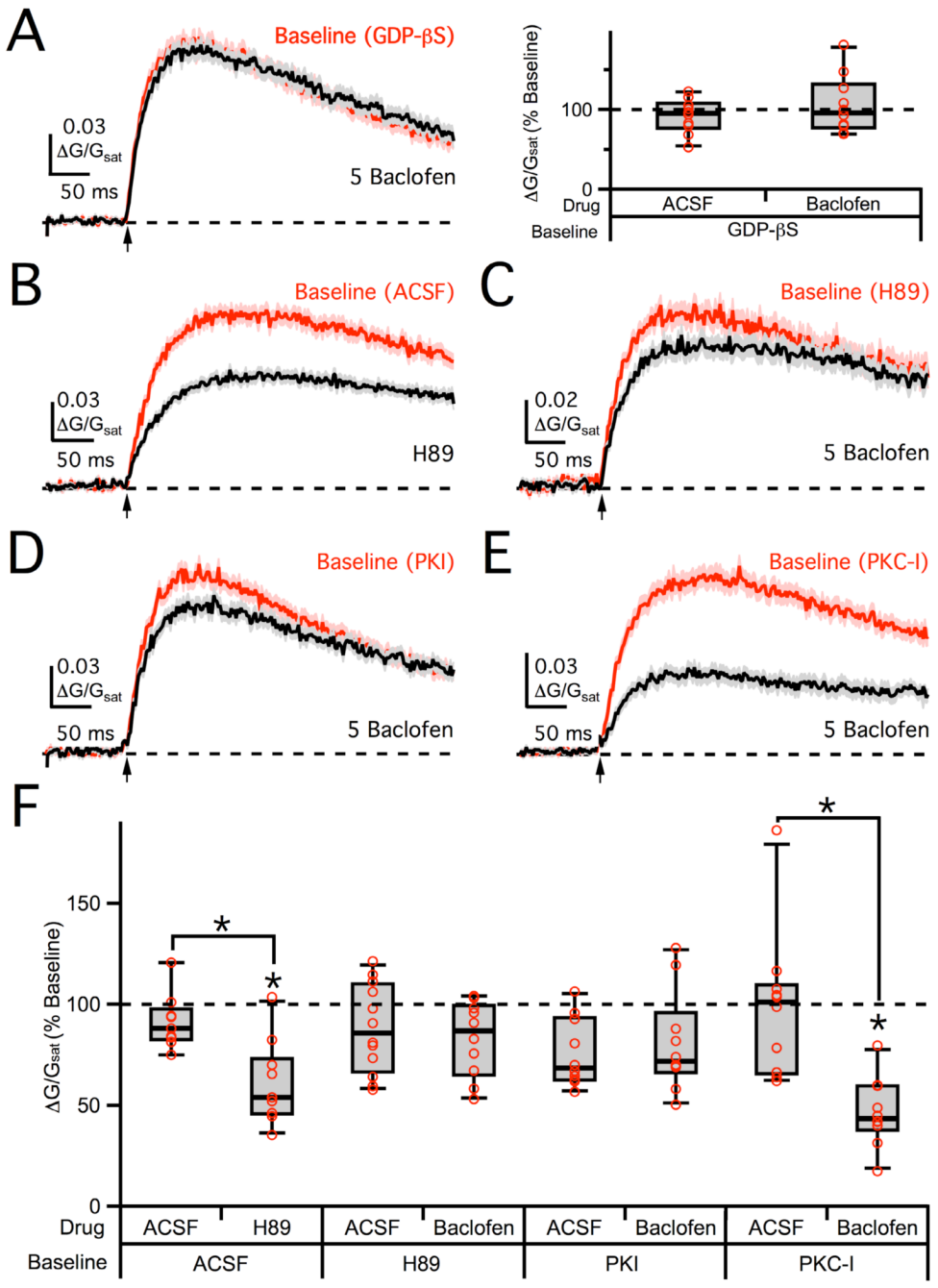

Figure 7. PKA mediates NMDA-R modulation

A, *Left*, Average 2PLU-evoked NMDA-R Ca signals in internal GDP-βS (*red*) and following wash-in of 5 μM baclofen (*black*). *Right*, Summary of changes in NMDA-R Ca signal amplitude following wash-in of baclofen or ACSF in GDP-βS. **B**, Average NMDA-R Ca signals in baseline ACSF (*red*) and following wash-in of H89 (*black*). **C**, Average NMDA-R Ca signals in bath-applied H89 (*red*) and following wash-in of 5 μM baclofen (*black*). **D**, Average NMDA-R Ca signals in internal PKI (*red*) and following wash-in of 5 μM baclofen (*black*). **E**, Average NMDA-R Ca signals in internal PKC-I (*red*) and following wash-in of 5 μM baclofen (*black*). **F**, Summary of changes in NMDA-R Ca signal amplitude following wash-in of drugs or vehicle controls in the different recording conditions. Asterisks indicate

significant ($P < 0.05$) difference from 100% or between different conditions. See also Figure S2.

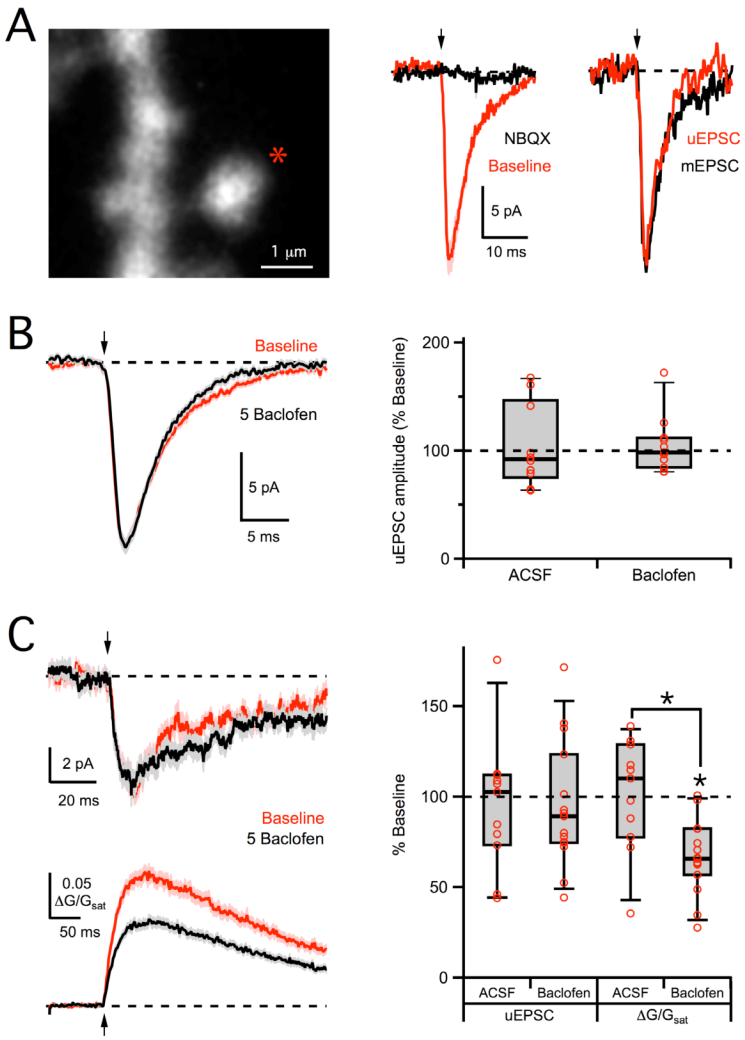

Figure 8. No modulation of AMPA-R or NMDA-R uEPSCs

A, *Left*, 2PLSM image of dendrite and spine, showing the uncaging location (*star*). *Middle*, 2PLU (*arrow*) evokes an AMPA-R uEPSC at −70 mV (*red*) that is blocked by wash-in of NBQX (*black*). *Right*, Average AMPA-R uEPSC (*red*) is similar to average miniature EPSC recorded in the same cell (*black*). **B**, *Left*, Average AMPA-R uEPSCs in baseline conditions (*red*) and following wash-in of 5 μM baclofen (*black*). *Right*, Summary of changes in AMPA-R uEPSC amplitude following wash-in of baclofen or ACSF. **C**, *Left*, Average NMDA-R uEPSCs (*top*) and Ca signals (*bottom*), recorded at −70 mV in 0 mM extracellular Mg, in baseline conditions (*red*) and following wash-in of 5 μM baclofen (*black*). *Right*, Summary of changes in NMDA-R uEPSC and Ca signal amplitudes following wash-in of baclofen or ACSF. Asterisks indicate significant ($P < 0.05$) difference from 100% or between different conditions. See also Figure S3.